Structure of $LaMo_2O_5$ Containing Both Isolated Mo_6O_{18} Clusters and Sheets of Fused Triangular Mo_3 Clusters

Simon J. Hibble,*,† Steven P. Cooper,† Alex C. Hannon,‡ Saban Patat,§ and William H. McCarroll||

Department of Chemistry, University of Reading, Whiteknights, Reading, RG6 6AD, U.K., ISIS Facility, Rutherford Appleton Laboratory, Chilton, Didcot, Oxon OX11 0QX, U.K., Department of Chemistry, Faculty of Arts and Science, University of Erciyes, Tr-38039 Kayseri, Turkey, and Chemistry Department, Rider College, 2083 Lawrenceville Road, Lawrenceville, New Jersey 08648

Received March 20, 1998

The structure of the disordered lanthanum molybdate, $LaMo_2O_5$, has been solved and refined using powder neutron diffraction data collected at 300 K. The average structure is described in $P6_3/mmc$, $a = 8.373(1)$ Å, $c = 19.1510(1)$ Å, $Z = 12$. The compound contains two types of Mo−Mo bonded units: isolated octahedral Mo_6O_{18} clusters, and infinite molybdenum oxide sheets, formed from condensed triangular Mo_3O_{13} clusters joined together to give a total of four Mo−Mo bonds for each molybdenum. The Mo_6O_{18} clusters have 16 electrons available for metal−metal bonding and the Mo−Mo distances within the unit are 2.643(4) Å × 6 and 2.695(5) Å × 6. In the infinite sheets the molybdenum−molybdenum distances are 2.612(9) Å within one equilateral triangular cluster and 2.621(8) Å within another. Each of the molybdenum atoms in the two different Mo_3 clusters has two molybdenum neighbors from the other cluster at a distance of 2.882(6) Å. Disorder in this layered structure occurs because of interchange of layers of Mo sheets with layers of lanthanum ions. The Bragg scattering is accounted for by including layers occupied with a 50% probability by each of these structural elements and their associated oxygen atoms. A model showing how ordered subunits are stacked together to produce the average structure is presented. Extended X-ray absorption fine structure spectroscopy (EXAFS) at the Mo K-edge was used to give information on the local structure around molybdenum and to confirm that the final structural model gives a good description of Mo−O and Mo−Mo bonding.

Introduction

There is a widespread interest in metal−metal bonding and the reduced molybdates provide a large range of compounds containing a variety of Mo−Mo bonded units.[1] The compound $Zn_2Mo_3O_8$,[2,3] which contains a Mo_3O_{13} metal−metal bonded cluster with $d_{Mo-Mo} = 2.524$ Å, is the archetype of these materials. Other cluster types include those containing Mo_4 units,[4] Mo_8 units,[5] and Mo_{10} units.[6] The Mo_6 cluster is a common structural unit but it is most frequently found fused to other such units to form chains; for example in KMo_4O_6 infinite Mo_4O_6 chains are formed.[7] In $BaMo_6O_{10}$, Mo_6 clusters are joined by intercluster Mo−Mo bonds to form a zigzag linking of clusters[8] and the only known example of an isolated Mo_6O_{18} cluster, Figure 1, is in $Ca_{16.5}Mo_{13.5}O_{40}$.[9]

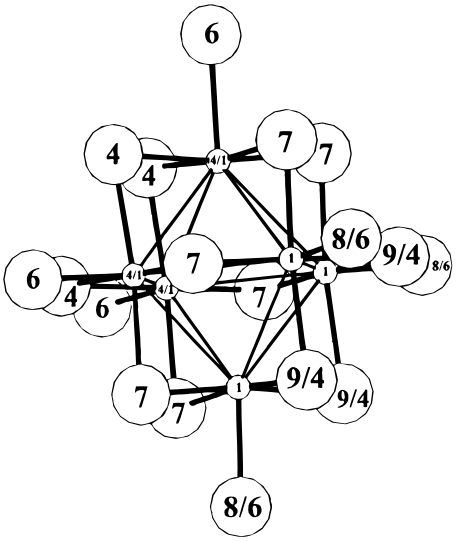

Figure 1. The Mo_6O_{18} unit (solid circles, Mo; open circles, O), atom labels are in the form model 1/model 2, where the numbering is different in the two models in Tables 1 and 4.

There is a great contrast between the types and numbers of metal−metal bonded clusters found in reduced molybdates[1] and those found in reduced niobates[10] and tungstates. In niobates,

† University of Reading.
‡ Rutherford appleton Laboratory.
§ University of Erciyes.
|| Rider College.

(1) Chippindale, A. M.; Cheetham, A. K. The Oxide Chemistry of Molybdenum. In *Studies in Inorganic Chemistry. Molybdenum: An Outline of its Chemistry and Uses*; Braithwaite, E. R., Haber, T., Eds.; Elsevier: Amsterdam, Netherlands, 1994.
(2) McCarroll, W. H.; Katz, L.; Ward, R. *J. Am. Chem. Soc.* **1957**, *79*, 5410.
(3) Ansell, G. B.; Katz, L. *Acta Crystallogr.* **1966**, *21*, 482
(4) Torardi, C. C.; Calabrese, J. C. *Inorg. Chem.* **1984**, *23*, 3281.
(5) Leligny, H.; Ledesert, M.; Labbe, Ph.; Raveau, B.; McCarroll, W. H. *J. Solid Sate Chem.* **1990**, *87*, 35.
(6) Hibble, S. J.; Cheetham, A. K.; Bogle, A. R. L.; Wakerley, H. R.; Cox, D. E. *J. Am. Chem. Soc.* **1988**, *110*, 3295.
(7) Torardi, C. C.; McCarley, R. E. *J. Am. Chem. Soc.* **1979**, *101*, 3963.
(8) Lii, K.-H.; Wang, C. C.; Wang, S. L. *J. Solid State Chem.* **1988**, *77*, 407.

10.1021/ic980313j CCC: $15.00
Published on Web 12/05/1998

metal−metal bonding is common and the Nb_6O_{18} cluster is the most frequently occurring cluster. However, clusters are exceedingly rare in tungstate chemistry in absolute numbers, and only two types are known. The octahedral W_6O_{18} cluster is known only in $Sn_{10}W_{16}O_{44}$,[11] and the W_3O_{13} cluster found only in metastable $Zn_2W_3O_8$[12] and the mixed metalates $Zn_2Mo_{3-x}W_xO_8$ with $x < 2$.[12,13]

Attempts have been made to rationalize the structure of these metal−metal bonded clusters in terms of electron count.[14] The isolated M_6O_{18} cluster is predicted to be most stable with 14−16 electrons per M_6 cluster. The only known Mo_6O_{18} example (in $Ca_{16.5}Mo_{13.5}O_{40}$[9]) appears to contain 17 electrons from bond order calculations, although there are uncertainties in the stoichiometry of this material. In the reduced niobates the isolated Nb_6O_{18} unit most often has an electron count of 14, for example in $Mg_3Nb_6O_{11}$[15] and $SrNb_8O_{14}$,[16] but electron counts of 13−15 are known.[10] The electron count for the octahedral W_6O_{18} cluster in $Sn_{10}W_{16}O_{44}$ is 14.[11]

The reduced molybdate $LaMo_2O_5$ was first prepared by McCarroll[17] using conventional solid-state synthetic methods in 1977 and later by fused salt electrolysis.[18] Single-crystal X-ray diffraction studies by McCarroll[18] and subsequent refinements by Thomas[19] appeared to show that $LaMo_2O_5$ contained Mo_6O_{18} clusters, but the structure has never been well enough determined to justify publication in the scientific press. It was thought that the problem with the structure determination might be caused by twinning. The easy twinning of this compound is probably a result of the layer structure of the compound. We decided to carry out a powder neutron diffraction study, for which twinning should present no problem and also to collect Mo K-edge extended X-ray absorption fine structure (EXAFS) data in order to determine the local structure around molydenum in this material.

Experimental Section

Synthesis. Lanthanum molybdate. $LaMo_2O_5$ was prepared by heating a mixture of Mo powder (Aldrich), MoO_2, and La_2O_3 (Aldrich) in the required stoichiometric quantities at 1225 °C for 72 h in an alumina tube contained inside a sealed evacuated silica ampule. The MoO_2 precursor was synthesized from Mo powder and MoO_3 (Aldrich) heated together at 500 °C for 24 h followed by a further 24 h at 1000 °C in a sealed evacuated silica ampule.

Neutron Scattering Data Collection. Time-of-flight powder neutron diffraction data were collected on the POLARIS diffractometer at the ISIS facility, Rutherford Appleton Laboratory (Chilton, Didcot, U.K.). A 5.23 g sample of powdered $LaMo_2O_5$ was loaded into a cylindrical thin-walled vanadium sample holder of nominal diameter 11 mm.

EXAFS Data Collection. Mo K-edge EXAFS data were collected in transmission mode on station 9.2 at the Daresbury Laboratory SRS, with an electron beam energy of 2 GeV and an average beam current of 130 mA. The silicon (220) double crystal order sorter monochromator was adjusted to give 50% harmonic rejection. Ionization chambers, filled with a mixture of Ar/He and Xe/He at appropriate partial pressures to optimize detector sensitivities, were placed in the beam path before and behind the sample. Finely ground samples were spread on Sellotape, and the number of layers was adjusted to give satisfactory absorption before and after the edge, and to maximize the change in absorption across the edge. The sample was cooled to around 80 K using a liquid nitrogen cooled sample holder in order to increase the magnitude of the EXAFS signal, especially at high k.

Table 1. Atom Parameters from Rietveld Refinement for $LaMo_2O_5$ (Model 1, $P6_3mc$ Structure)[a]

atom	multiplicity	x	y	z	B/Å^2	occupancy
La1	6	0.5203(9)	0.4797(9)	0.848(2)	1.3(2)	1.0
La2	2	0.0000	0.0000	0.246[b]	1.3(2)	1.0
La3	2	1/3	2/3	0.990(2)	1.3(2)	1.0
La4	2	1/3	2/3	0.504(2)	1.3(2)	1.0
Mo1	6	0.111(1)	0.889 (1)	0.942(2)	0.20 (6)	1.0
Mo2	6	0.769(1)	0.231(1)	0.681(2)	0.20 (6)	1.0
Mo3	6	0.562(1)	0.438(1)	0.177(2)	0.20 (6)	1.0
Mo4	6	0.892(1)	0.108(1)	0.058(2)	0.20 (6)	1.0
O1	12	0.325(1)	0.994(1)	0.247(2)	0.19(4)	1.0
O2	2	1/3	2/3	0.235(2)	0.19(4)	1.0
O3	2	1/3	2/3	0.759(2)	0.19(4)	1.0
O4	6	0.104(1)	0.208(2)	0.123(2)	0.19(4)	1.0
O5	6	0.556(1)	0.112(3)	0.614(2)	0.19(4)	1.0
O6	6	0.448(3)	0.224(1)	0.106(2)	0.19(4)	1.0
O7	12	0.015(3)	0.342(1)	0.993(2)	0.19(4)	1.0
O8	6	0.450(2)	0.225(1)	0.389(2)	0.19(4)	1.0
O9	6	0.113(1)	0.226(3)	0.374(2)	0.19(4)	1.0
O10	2	1/3	2/3	0.386(2)	0.19(4)	1.0

[a] $a = 8.37(4)$ Å, $c = 19.1484(1)$ Å. Number of reflections used = 397, $\chi^2 = (R_{wp}/R_{ex})^2 = 172$ for 2128 observations and 42 basic variables, $R_{wp} = [\Sigma_i w_i |I_{obs,i} - I_{calc,i}|^2/\Sigma_i w_i I_{obs,i}^2]^{1/2} = 0.0857$, $R_{ex} = [(N - P + C)/\Sigma_i w_i I_{obs,i}^2]^{1/2} = 0.0066$; R_{wp} is the weighted profile R factor, R_{ex} is the expected R factor, w_i is the weight for point i, N = no. of observations, $I_{obs,i}$ and $I_{calc,i}$ are the observed and calculated intensities of point i, P = no. of variables, and C = no. of constraints. [b] The z parameter of La(2) is fixed to define the origin.

Data Reduction and Analysis. (a) Rietveld Analysis. Data from the POLARIS C-bank detectors, at angles 130−158°, which gives the highest resolution, were used for the refinement. The data from individual detectors were focused, summed and normalized to the incident neutron spectrum to produce a diffraction pattern over the time-of-flight range (tof), 2500−19600 μs (d spacing range 0.404−3.177 Å). Standard Rietveld refinements for $LaMo_2O_5$ were carried out using the program TF14LS,[20] over the tof range 5300−19000 μs (d range 0.858−3.079 Å) with the peak shape modeled by a pseudo-Voigt function convoluted with a double exponential function. The coherent scattering lengths used for La, Mo, and O were 0.824×10^{-14} m, 0.6715×10^{-14}, and 0.5803×10^{-14}, respectively.[21]

(b) EXAFS Data Analysis. The programs EXCALIB, EXBACK, and EXCURV92[22] were used to extract the EXAFS signal and analyze the data. A background subtraction was carried out by linear extrapolation of the preedge region. In the conversion of the data to k space, E_0 was defined as the maximium change of gradient of the edge region and determined by studying the first derivative of the spectrum. We chose the Hedin−Lundqvist method to calculate the exchange potentials, which takes account of the mean free path losses and core hole broadening, and the von Bart method to calculate the ground-state potentials used in this work. No correction was applied to account for monochromator resolution. The excited atom was treated using the "Z+1" approximation in the calculation of theoretical phase-shifts; this was carried out within EXCURV92[22] The Fourier transform presented was calculated using a Gaussian window and the phase shift calculated for the oxygen shell.

(9) Lindblom, B.; Strandberg, R. *Acta Chem. Scand*. **1989**, *43*, 825.
(10) Köhler, J.; Svensson G.; Simon A. *Angew. Chem., Int. Ed. Engl.* **1992**, *31*, 1437.
(11) Hibble, S. J.; McGrellis, S. A. *J. Chem. Soc., Dalton Trans.* **1995**, 1947.
(12) Tourne, G.; Czeskleba, H. *C. R. Seances Acad. Sci.* **1970**, *C271*, 136.
(13) Hibble, S. J.; Fawcett, I. D. *J. Chem. Soc., Dalton Trans.* **1995**, 2555.
(14) Simon, A. *Angew. Chem., Int. Ed. Engl.* **1988**, *27*, 159.
(15) Marinder, B.-O. *Chem. Scr*. **1977**, *11*, 97.
(16) Köhler, J.; Simon, A.; Hibble, S. J.; Cheetham, A. K. *J. Less Common Metals* **1988**, *142*, 123.
(17) McCarroll, W. H.; Darling, C. M.; Jakubicki, G. *J. Solid State Chem.* **1983**, *48*, 189.
(18) McCarroll, W. H. Unpublished research.
(19) Thomas, D. M. D.Phil. University of Oxford, U.K., 1986.
(20) David, W. I. F.; Ibberson, R. M.; Matthewman, J. C. *Rutherford Appleton Laboratory Report, RAL-92-032*; Chilton, Didcot, Oxon, U.K., 1992.
(21) Sears, V. F. *Neutron News* **1992**, *3*, 26.
(22) Binsted, N.; Campbell, J. W.; Gurman, S. J.; Stephenson, P. C. *EXAFS data analysis program*; Daresbury Laboratory: Daresbury, U.K., 1991.

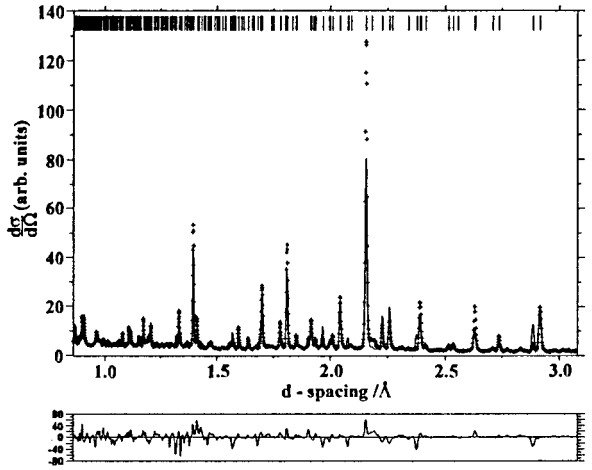

Figure 2. Final fitted profiles (points, observed; line, calculated; lower, $((I_{obs} - I_{calc})/esd)$) from Rietveld refinement for $LaMo_2O_5$ using the model in space group $P6_3mc$. Tick marks directly above the diffraction pattern indicate the positions of the allowed reflections.

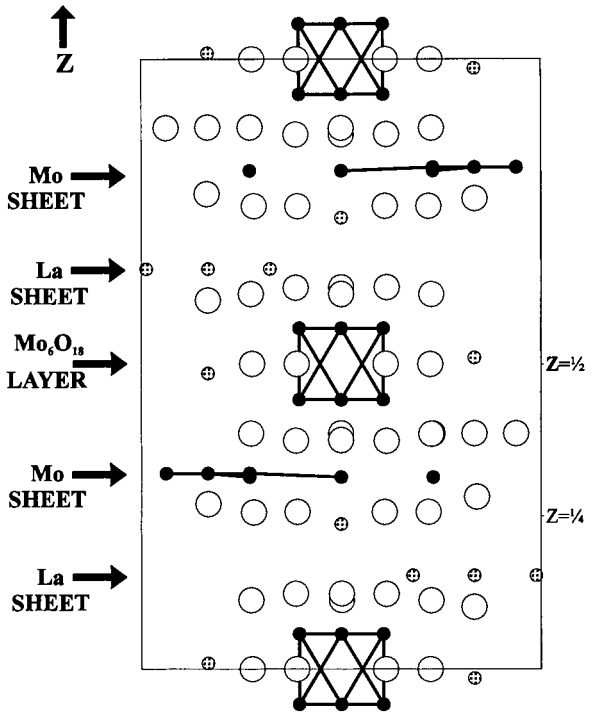

Figure 3. Structural model for $LaMo_2O_5$ (model 1) in space group $P6_3mc$ projected down the [120] direction (solid circles, Mo; open circles, O; spotted circles, La), only Mo−Mo bonds are shown, light lines indicate the unit cell.

Results of Modeling

Model 1. The atomic parameters of Thomas[19] in space group $P6_3mc$ were used as a starting point for the Rietveld refinements. The scale factor and 10 polynomial background parameters were refined first, followed by the unit cell, the atomic parameters, one isotropic temperature factor for each of the three atom types, La, Mo, and O, and finally the peak shape parameters. The refined lattice and atomic parameters from this refinement are given in Table 1. For ease in comparing the structural models *z* for La(2) has been fixed at 0.246 rather than 0.0 in the Thomas model; this places the origin close to the center of a Mo_6O_{18} cluster. The observed and calculated intensities (I_{obs} and I_{calc}) and the difference/estimated error plot ($(I_{obs} - I_{calc})/esd$ where esd is the standard deviation on I_{obs} determined from counting statistics) for Model 1 are shown in Figure 2. Figure 3 shows a projection of the structure of $LaMo_2O_5$ in which the layers containing Mo_6O_{18} clusters, the infinite metal−metal bonded molybdenum sheets, and the lanthanum-only layers are labeled. The Mo_6O_{18} unit has been shown already in Figure 1, while Figure 4 shows a more extended view of the infinite Mo sheet.

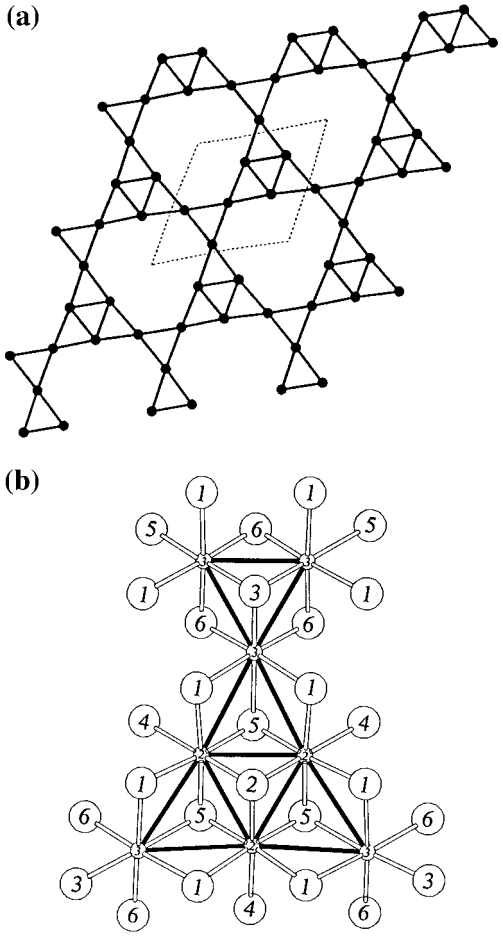

Figure 4. (a) An extended view of the infinite Mo−Mo bonded sheets present in $LaMo_2O_5$, light lines indicate the unit cell. (b) A section of this Mo−Mo bonded sheet with attached oxygens (solid circles, Mo; open circles, O), atom labels correspond to those in Tables 1 and 4.

Table 2. Selected Interatomic Distances (Å) in $LaMo_2O_5$ ($P6_3mc$ Structure, Model 1) with Esd's in Parentheses

La(1)−O(1)×2	2.42(4)	Mo(1)−Mo(1)×2	2.79(2)
O(2)	3.03(4)	Mo(4)×2	2.73(4)
O(3)	3.20(3)	O(7)×2	1.85(4)
O(7)×2	3.13(5)	O(8)	1.94(3)
O(9)×2	2.86(2)	O(9)×2	2.08(4)
O(10)	2.24(2)	Mo(2)−Mo(2)×2	2.57(2)
La(2)−O(1)×6	2.75(1)	Mo(3)×2	2.88(1)
O(4)×3	2.80(3)	O(1)×2	2.07(3)
O(9)×3	2.95(3)	O(2)	1.81(3)
La(3)−O(5)×3	2.56(4)	O(4)	2.15(3)
O(7)×6	2.71(3)	O(5)×2	2.01(4)
O(8)×3	2.80(4)	Mo(3)−Mo(3)×2	2.63(2)
La(4)−O(6)×6	2.52(4)	Mo(2)×2	2.88(1)
O(7)×3	2.89(2)	O(1)×2	2.18(4)
O(10)×3	2.26(5)	O(3)	2.18(4)
		O(5)	2.09(4)
		O(6)×2	2.06(4)
		Mo(4)−Mo(4)×2	2.71(2)
		Mo(1)×2	2.73(2)
		O(4)×2	1.98(4)
		O(6)	1.92(3)
		O(7)×2	2.11(4)

Table 3. Coordination Numbers (N), Distances (R), and σ, the Root Mean Squared Variation in Bond Length Derived from the Mo K-Edge EXAFS Studies of $LaMo_2O_5$[a]

shell	N	R/Å	σ/Å
O	5.5	2.035(3)	0.063(4)
Mo	4.0	2.668(2)	0.077(1)
Mo	2.3	3.75(5)	0.067(3)
La	2.8	3.723(4)	0.13(1)

[a] Nine independent parameters (indicated by the figures with estimated standard deviations in brackets plus the Fermi energy) were refined to fit the EXAFS over the k range 3.00−17.84 Å^{-1}, yielding $R = (\int|(\chi^T(k) - \chi^E(k))|k^3\, dk/\int|\chi^E(k)|k^3\, dk) = 0.353$ where $\chi_i^T(k)$ and $\chi_i^E(k)$ are the theoretical and experimental EXAFS, respectively. Errors quoted are statistical errors from least-squares refinements.

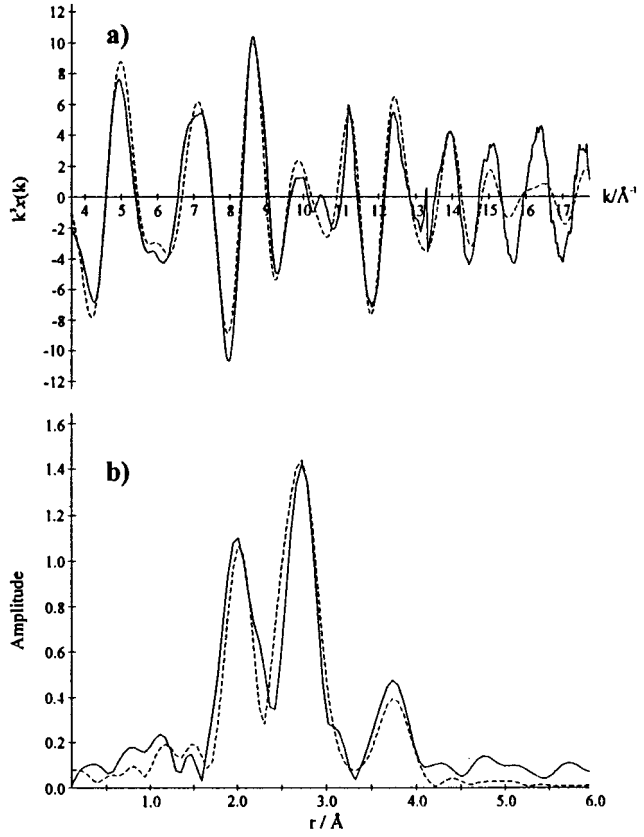

Figure 5. Molybdenum K-edge EXAFS data for $LaMo_2O_5$ collected at 80 K. (a) k^3 weighted EXAFS, (—) experimental and (- -) theoretical, and (b) the Fourier transform.

Table 2 gives a list of important interatomic bond distances obtained from this refinement.

This model gives quite a high weighted profile R factor (R_{wp}) of 0.0857, but the basic structure appears chemically sensible. However, a number of problems remain as can be seen if the bond order sums around oxygen atoms are calculated. Molybdenum−oxygen bond orders (s_{Mo-O}) for a molybdenum to oxygen bond of length R were calculated using $s_{Mo-O} = (R/R_1)^{-6}$ with $R_1 = 1.882$ (for a bond order of 1), and lanthanum−oxygen bond orders (s_{La-O}) for lanthanum oxygen bond of length R were calculated using $s_{La-O} = (R/R_1)^{-6.5}$ with $R_1 = 2.167$ (for a bond order of 1).[23] Using the Mo−O and La−O bond distances in Table 2 the bond order sum around some of the oxygens yield physically unreasonable values. For example, O(3), which caps an $Mo(3)_3$ triangle (see Figure 4b), yields a value of 1.48, and O(2), which caps an $Mo(2)_3$ triangle

(23) Brown, I. D.; Wu, K. K. *Acta Crystallogr.* **1976**, *B32*, 1957.

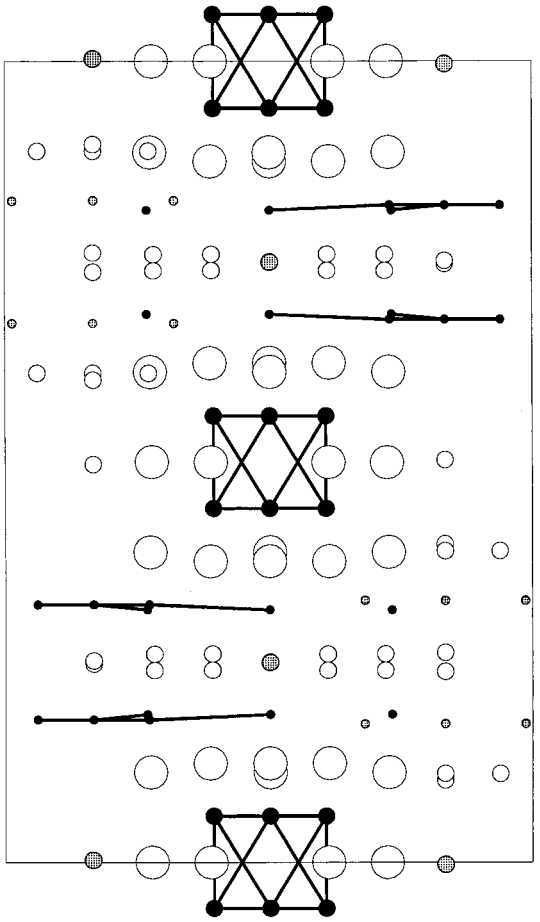

Figure 6. Average unit cell for $LaMo_2O_5$ projected viewed in the [120] direction (space group $P6_3/mmc$, solid circles, Mo; open circles, O; spotted circles, La. Small and large circles represent atoms with occupancies of 0.5 and 1, respectively), only Mo−Mo bonds are shown, light lines indicate the unit cell.

yields a value of 4.17, rather than the bond order of 2 expected for oxygen. These values show that this model falls short of providing a good description of the structure. In addition a Fourier difference map revealed significant scattering density in the layers containing the Mo and La sheets unaccounted for by this model. We now turned to EXAFS to give further information on the local structure in this material.

EXAFS Modeling. Using the basic structure determined above as a starting point, we fitted the molybdenum K-edge EXAFS signal using four shells, with the coordination number (N) fixed at the crystallographically determined value. The results are given in Table 3, and the fitted EXAFS and Fourier transform are shown in Figure 5. The most revealing information comes from the parameters obtained for the oxygen shell. This shell is particularly well characterized; if N for the oxygen shell is refined together with the four distances (R) and the root-mean-squared variation (σ) in R for each of the four shells a value of 5.4 is obtained for the Mo−O coordination number. This value is hardly changed from the average value of 5.5 determined crystallographically, and well within the errors expected from an EXAFS determination. We fixed N for the oxygen shell at 5.5 in the final refinement to allow a meaningful comparison of the variations in Mo−O bond lengths determined by diffraction and EXAFS to be made. The average Mo−O distance of 2.039 Å compares very well with the value, 2.035 Å, obtained from the Rietveld refinement. However, the value (see Table 3) of the total disorder in the oxygen shell measured

Table 4. Atom Parameters from Rietveld Refinement for $LaMo_2O_5$ ($P6_3/mmc$ Structure, Model 2)[a]

atom	multiplicity	x	y	z	B/Å^2	occupancy
La1	12	0.5122(5)	0.4878(5)	0.8459(4)	1.26(9)	0.5
La2	4	0.0000	0.0000	0.2387(6)	1.26(9)	0.5
La3	4	$^1/_3$	$^2/_3$	0.9850(7)	1.26(9)	0.5
La4	4	$^1/_3$	$^2/_3$	0.0098(8)	1.26(9)	0.5
Mo1	12	0.1052(3)	0.8948(3)	0.9420(2)	0.34(8)	1.0
Mo2	12	0.7709(7)	0.2291(7)	0.6843(5)	0.34(8)	0.5
Mo3	12	0.5623(6)	0.4377(6)	0.1786(4)	0.34(8)	0.5
O1	24	0.3277(7)	0.000(8)	0.2422(4)	0.27(8)	0.5
O2	4	$^1/_3$	$^2/_3$	0.2642(4)	0.27(8)	0.5
O3	4	$^1/_3$	$^2/_3$	0.751(6)	0.27(8)	0.5
O4	12	0.1137(4)	0.2274(7)	0.1243(2)	0.27(8)	1.0
O5	12	0.5620(8)	0.1238(16)	0.6130(5)	0.27(8)	0.5
O6	12	0.4513(9)	0.2257(4)	0.1135(3)	0.27(8)	1.0
O7	12	0.0000	0.3339(7)	0.0000	0.27(8)	1.0
O10	4	$^1/_3$	$^2/_3$	0.3972(7)	0.27(8)	0.5

[a] $a = 8.373(1)$ Å, $c = 19.1510(1)$ Å. Number of reflections used = 397, $\chi^2 = 20$ for 2128 observations and 39 basic variables, $R_{wp} = 0.0289$, $R_{ex} = 0.0064$.

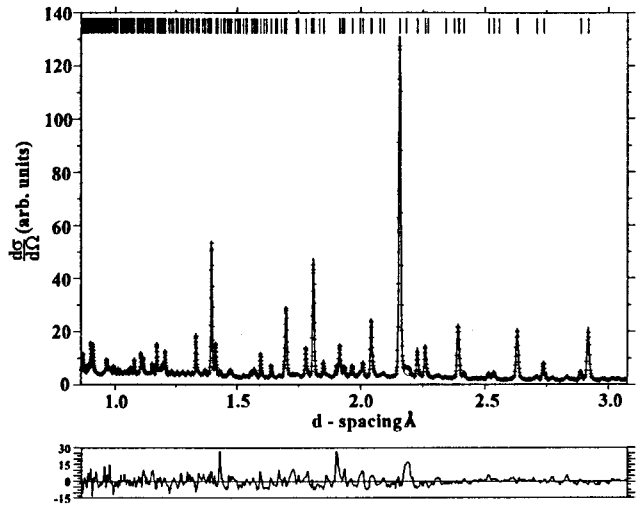

Figure 7. Final fitted profiles (points, observed; line, calculated; lower, $((I_{obs} - I_{calc})/esd)$) from the Rietveld refinement for $LaMo_2O_5$ using the disordered model in space group $P6_3/mmc$. Tick marks directly above the diffraction pattern indicate the positions of the allowed reflections.

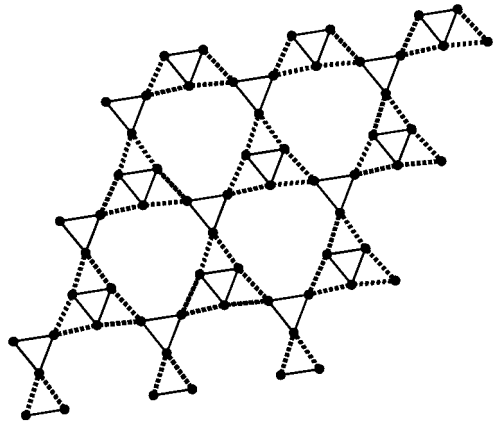

Figure 8. An alternative view of the molybdenum sheets present in $LaMo_2O_5$ (bold lines indicate bonds with d(Mo−Mo) < 2.7 Å; dashed lines indicate d(Mo−Mo) > 2.85 Å).

as the root-mean-square variation, $\sigma_{total} = 0.063$ Å, is much lower than that, $\sigma_{static} = 0.106$ Å, calculated using only static disorder from the model obtained by neutron profile refinement. The difference is especially striking when one considers that σ_{total} from the EXAFS experiment contains a thermal contribution, albeit reduced by carrying out the experiment at 80 K. The low root-mean-squared displacement in Mo−O distances was initially surprising, since we expected that we would need to add disorder to our model to better account for the observed diffraction pattern. One possible explanation is that $LaMo_2O_5$ contains regular structural units that are disordered, rather than units which are disordered in themselves and we now attempt to construct a model including this feature.

Table 5. Selected Interatomic Distances (Å) in $LaMo_2O_5$ ($P6_3/mmc$ Structure, Model 2) with Esd's in Parentheses; Distances Correspond to Local Rather than Average Structure

La(1)−O(1)×2	2.461(9)	Mo(1)−Mo(1)×2	2.695(5)
O(2)	2.733(8)	Mo(1)×2	2.643(4)
O(3)	3.190(9)	O(4)×2	2.036(5)
O(4)×2	2.891(5)	O(6)	2.045(8)
O(6)×2	2.392(9)	O(7)×2	1.998(3)
O(7)×2	3.267(7)	Mo(2)−Mo(2)×2	2.612(9)
O(10)	2.446(8)	Mo(3)×2	2.882(6)
La(2)−O(1)×6	2.768(5)	O(1)×2	2.003(9)
O(4)×3	2.74(1)	O(2)	2.15(1)
O(4)×3	3.098(3)	O(4)	2.03(1)
La(3)−O(7)×6	2.804(3)	O(5)×2	2.04(1)
O(6)×3	2.44(1)	Mo(3)−Mo(3)×2	2.621(8)
O(10)	2.26(2)	Mo(2)×2	2.882(6)
La(4)−O(5)×3	2.49(1)	O(1)×2	2.093(9)
O(6)×3	2.83(1)	O(3)	2.03(1)
O(7)×6	2.795(3)	O(5)	2.20(1)
		O(6)×2	1.980(9)

Model 2. Inspection of model 1 shows that a pseudocenter of symmetry can be found at the center of the Mo_6O_{18} cluster (see Figure 1). If this center of symmetry is added the atom pairs Mo(1) and Mo(4), O(4) and O(9), and O(6) and O(8) become equivalent and only one of each pair is needed to describe this unit. We constructed a model containing these more regular Mo_6O_{18} octahedral clusters by adding a center of symmetry to the space group $P6_3mc$ to give space group $P6_3mmc$. We removed one of each of the pairs of atoms mentioned above, and placed La(2), O(1), O(2), and O(3) on the mirror plane at $z = {}^1/_4$. This approach does not at first appear promising, since the remaining atoms from model 1 produce physically unreasonable structural elements and the wrong composition. The most obvious problem is that the number of molybdenum sheets and La(1), La(3), and La(4) atoms are doubled and many unreasonable Mo−Mo, La−La, and La−Mo contacts are produced. However, this initially unappealing model can be accounted for if the extra lanthanum layers (La(1)), the molybdenum sheets (Mo(2) and Mo(3)) along with two of the associated oxygens O(5) and O(10), and La(3) and

Table 6. Motifs of Mutual Adjunction,[24] Coordination Numbers (CN), and Bond Order Sums[23] (Σs_i) in $LaMo_2O_5$[a]

atom	O(1)	O(2)	O(3)	O(4a)	O(4b)	O(4c)	O(4d)	O(5a)	O(5b)	O(6a)	O(6b)	O(6c)	O(6d)	O(7a)	O(7b)	O(7c)	O(10)	CN	Σs_i
Mo(1a)				2/2						1/1					2/2			5	3.26
Mo(1b)					2/2						1/1					2/2 OR		5	3.26
Mo(1c)						2/2						1/1				2/2		5	3.26
Mo(1d)							2/2						1/1	2/2				5	3.26
Mo(2)	2/1	1/3		1/1 or 1/1				2/2 or 2/2										6	3.69
Mo(3)	2/1		1/3					1/1 or 1/1		2/2 or 2/2								6	3.67
La(1)	2/1	1/3	1/3			2/2 or 2/2						2/2 or 2/2		2/2	or	2/1	1/3	11	3.13
La(2)	6/1			3/1 or 3/1		3/1 or 3/1												12	2.17
La(3a)										3/1 or 3/1						6/1	1/1	10	3.29
La(3b)										OR	OR	3/1 or 3/1		6/2			1/1	10	3.29
La(4a)									3/1	3/1 or 3/1		OR	OR		6/2			12	2.88
La(4b)								3/1				3/1 or 3/1				6/1		12	2.88
CN	4	6	6	4	4	5	5	4	4	4	4	4	4	6	4	5	4		
Σs_i	1.92	2.01	2.17	1.98	1.98	1.77	1.77	2.03	2.03	2.20 OR	2.20 OR	2.12 OR	2.12 OR	1.91	1.78	1.70	2.15		
Σs_i										2.26	2.26	1.84	1.84						

[a] Or is read horizontally and OR, vertically. [b] a, b, c, and d indicate different possibilities for local coordination of the atoms. The particular local coordination adopted depends on the actual occupation of the partially occupied La and Mo sheets shown in the average structure. Thus O(7c) occurs when the both the Mo sheets immediately adjacent to the layer occupied by the Mo_6O_{18} are occupied.

La(4) are only 50% occupied; Figure 6 shows this structure. Refinement of this model produced a much improved fit to the neutron powder diffraction pattern with R_{wp} falling to 0.0426. However, problems remained with high-temperature factors for oxygen and lanthanum atoms. It was clear from considering the bonding requirements of O(2) and O(3) that they would be expected to be displaced in the *z* direction to lie closer to whichever of the layers was occupied by the Mo sheet and away from the La sheet. We therefore moved atoms O(2) and O(3) off the mirror plane and gave them half occupancy. Refinement produced a structure which yielded much more physically reasonable bond-order sums around O(2) and O(3) and R_{wp} fell to 0.0315. We then displaced O(1), the remaining oxygen on the mirror plane at $z = {}^1/_4$ and gave it 50% occupancy. This also led to both an improvement in R_{wp} (R_{wp} fell to 0.0302) and in the chemical plausability of the structure. The final step was to carry out the same procedure for La(2). Splitting the La(2) site produced a large drop in the La temperature factor and an increase in the La(2)−O bond order sum from 2 to 2.17, moving closer to the expected value of 3, but still rather low. The final weighted profile *R* factor was $R_{wp} = 0.0289$. The final atomic parameters are given in Table 4, and the final fitted profile is shown in Figure 7. A projection of the final average structure is shown in Figure 8 with the partially occupied atomic sites indicated. Care has to be taken when calculating interatomic distances from an average structure, for example, if the La(4) site is occupied the adjacent O(10) is unoccupied, but O(5) is present. Similarly, when calculating Mo−O bond orders for molybdenum atoms in the sheets, the Mo−O distances taken must be to the oxygens which will be present when that particular sheet is occupied. Important bond distances for this model are given in Table 5, taking account of the local coordination derived from the average structure using these constraints. To help to make clear the local coordination geometry in $LaMo_2O_5$, and give further insight into the structure, motifs of mutual adjunction,[24] and bond-order sums are given in Table 6, and are discussed further below. In Table 6 one reads along the row to determine which oxygens are connected to a particular metal atom, the first number in the entry under each oxygen type gives the number of oxygens of this type connected to this metal atom. Reading down the columns yields the number of metal atoms of a particular type connected to the oxygen at the head of the column, the second number in the entry against each type of metal atom gives the number of metal atoms of this type connected to this oxygen atom. To interpret Table 6 one must consider that different local structures can be envisaged as contributing to the average structure. These will produce different local connectivity and bond-order sums around atoms which are crystallographically identical in the average structure. We have indicated some of these possibilities by adding letters to the atom numbers to differentiate between different local atom types. The table includes all possibilities for different bond-order sums. Unfortunately, Table 6 would have to be infinite to describe all atoms in this disordered structure in terms of differences in the coodination of nearest, next nearest, ..., and further neighbors. We have included one example of next nearest neighbor connectivity to illustrate this point by showing the four possibilities for Mo(1).

Alternative Models. Other models can be constructed which would explain the Bragg scattering. However, these give physically nonsensical bond distances and bond orders. For example, taking isolated $[Mo(2)]_3$ triangles in one set of layers and $[Mo(3)]_3$ triangles in another, with La atoms acting as spacers, leads to La−Mo distances of 1.17 Å.

Discussion

The final weighted profile *R* factor ($R_{wp} = 0.0289$) for model 2 is very good and the atomic parameters in Table 4 give a good description of the average structure. The relatively high χ^2 of 20 is a result of the high intensity and good counting statistics for the data, which lead to very small expected statistical errors. The most notable discrepancies in the description of the Bragg scattering occur around *d* of 1.4, 1.9, and 2.2 Å. In each of these three regions the difference plot shows a peak which is broader than the peaks accounted for in our model. These peaks can be indexed on a larger hexagonal cell with *a* and *b* doubled from their present values. This suggests a still deeper level of structural complexity exists in this material. We have not attempted to tackle this more complex problem, since the structural model used here accounts for almost all the Bragg scattering and these weak peaks contain little extra information. In addition, the number of variables required to describe a structure with a unit cell volume four times that of the present model would be too large for Rietveld refinement.

There is very good agreement between the mean values of d_{Mo-O} found from the EXAFS and diffraction studies of 2.039

(24) Hoppe, R. *Angew. Chem., Int. Ed. Engl.* **1980**, *19*, 110.

and 2.035 Å, respectively. The value for the static variation, $\sigma_{static} = 0.050$ Å, in d_{Mo-O} derived from the diffraction data, is now as it should be, less than $\sigma_{total} = 0.063$ Å derived from EXAFS. An estimate of the contribution of thermal disorder to the variation, $\sigma_{thermal}$, in d_{Mo-O} to the EXAFS signal at 80 K can be made from our measurements on related model compounds.[13] These yield $\sigma_{thermal} = 0.032$ Å for the first Mo−O coordination shell, since $\sigma^2_{total} = \sigma^2_{static} + \sigma^2_{thermal}$ this yields $\sigma_{static} = 0.054$ Å for the static variation in d_{Mo-O} in excellent agreement with the value obtained from neutron diffraction. This suggests that the interatomic distances in Table 5 accurately describe the local structure around molybdenum. We therefore have some confidence in the bond order calculations for Mo−O bonds shown in Table 6. These are likely to be most accurate for the Mo_6O_{18} unit which is least affected by the disorder in the material.

The bond order sum, Σs_{Mo-O}, around Mo(1) is 3.26, giving a calculated electron count of 16.44 for this Mo_6O_{18} cluster and suggesting that this cluster has an electron count of 16. This is at the top end of the range of electron counts expected and corresponds to filling all the Mo−Mo bonding orbitals for the cluster. The value calculated using Mo−O bond order calculations for the Mo_6O_{18} cluster in $Ca_{16.5}Mo_{13.5}O_{40}$[9] is 16.89 compared with the value of 17 calculated from the formula if 1.5 of the Mo atoms are Mo^{VI}. Calculating the electron count for $Ca_{16.5}Mo_{13.5}O_{40}$ is, however, not straightforward, since the stoichiometry of the compound is uncertain. It is possible that this compound also contains Mo_6O_{18} clusters with 16 electrons involved in cluster bonding orbitals. The values found for the electron count of the Mo_6O_{18} clusters in $LaMo_2O_5$ and $Ca_{16.5}Mo_{13.5}O_{40}$ can be compared with the values found for Nb_6O_{18} clusters of 13−15 electrons per cluster,[10] and the value of 14 found for the W_6O_{18} cluster in $Sn_{10}W_{16}O_{44}$.[11] The Mo−Mo bond lengths found within the Mo_6O_{18} clusters in the two molybdenum compounds are similar. In $LaMo_2O_5$ there are 6 bonds of 2.643 Å and 6 bonds of 2.695 Å within the cluster, and in $Ca_{16.5}Mo_{13.5}O_{40}$ there are 8 bonds of 2.670 Å and 4 of 2.772 Å. Intercluster Mo−Mo distances in $LaMo_2O_5$ are greater than 3.5 Å, and are well outside the range for metal−metal bonding.

The bond order sums, Σs_{Mo-O}, around Mo(2) and Mo(3) (the molybdenum atoms forming the infinite sheets) give values of 3.69 and 3.67, respectively. Taking these values with the value for Mo(1) calculated above, and allowing for the different occupancies of the molybdenum atoms, yields an average oxidation state for molybdenum of 3.47, in excellent agreement with the formulation $La^{III}Mo_2(O^{2-})_5$. The Mo−Mo bonding around Mo(2) and Mo(3) can be viewed in two different ways: Figure 4 shows a view with all Mo−Mo distances of less than 2.9 Å shown as bonds giving a 4-connected net. In passing we note that this represents an infinite two-dimensional way in which four Mo−Mo bonds can form around each molybdenum while the Mo_6 octahedral cluster represents an isolated three-dimensional solution. Another representation of the infinite Mo sheet is given in Figure 8 where short Mo−Mo bonds ($d_{Mo-Mo} < 2.7$ Å) are shown as thick solid lines while the longer Mo−Mo bonds ($d_{Mo-Mo} = 2.88$ Å) are shown as double lines. This emphasizes the triangular Mo_3 clusters typical of Mo^{IV}.[1−3] The Mo−Mo distances in the $Mo(2)_3$ triangles and $Mo(3)_3$ triangles of 2.612 and 2.621 Å, respectively, are slightly longer than that of 2.524 Å found in $Zn_2Mo_3O_8$.[3] We might envisage that the extra electrons above the 6 required to fill the bonding orbitals of the Mo_3 clusters are used for further Mo−Mo bonding to adjacent clusters. A band structure calculation on this sheet would be interesting to give additional information on the degree of metal−metal bonding between the triangular clusters and to rule out the possibility that the longer Mo−Mo distances are not merely a result of contraints imposed by Mo−O bonding requirements.

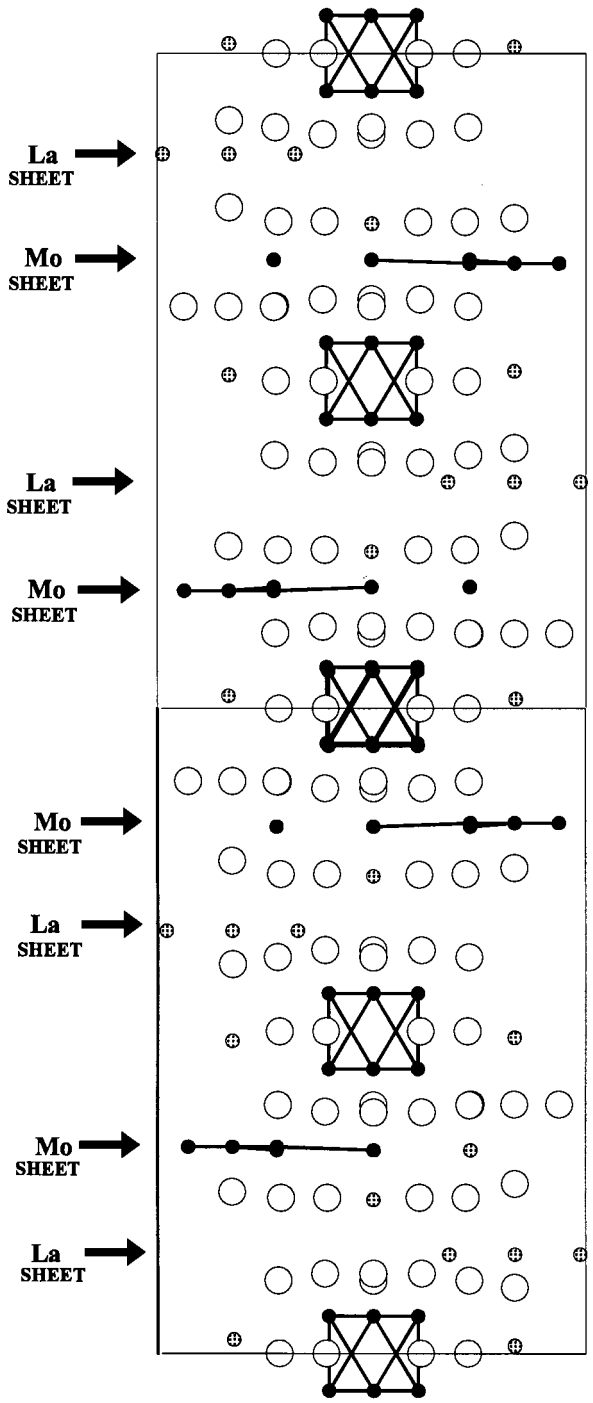

Figure 9. Projection (down the [120] direction) of one of the possible local structures in $LaMo_2O_5$, which contribute to the average structure (solid circles, Mo; open circles, O; spotted circles, La), only Mo−Mo bonds are shown, light lines indicate the individual units with $P6_3mc$ symmetry.

Although our principal motivation was to determine the types of Mo−Mo bonded clusters present (as described above) the bonding around the lanthanum atoms and their role in the structure of $LaMo_2O_5$ is also of interest. Our model gives reasonable bond order sums for La(1) and La(3) of 3.13 and 2.88, respectively. However, examination of the bond order sums

around La(2) suggests that the average structure might not produce a very good description of the bonding around this lanthanum. The lanthanum−oxygen bond-order sum around La(2) is 2.17, differing significantly from the expected value of 3. It is likely that in $LaMo_2O_5$ the molybdenum−oxygen framework has the dominant role in controlling the structural geometry, and that the lanthanum ions with their less rigid demands on coordination number and geometry move off ideal sites to accommodate the bonding requirements of oxygen. This conclusion is supported by the thermal displacement parameters from the Rietveld refinement (*B* in Table 4); the value for lanthanum is found to be substantially higher than the values for molybdenum or oxygen. It should be noted that such discrepancies in bond order sums and high thermal displacement parameters have been found for the countercations in other compounds containing metal−metal bonded clusters, for example strontium and barium in $SrNb_8O_{14}$ and $BaNb_8O_{14}$.[16,25] The case of $LaMo_2O_5$ is, however, more complicated than this example because of the disorder of the molybdenum sheets and lanthanum layers.

The average structure can be envisioned as being made up by connecting the unit cell shown in Figure 2 (model 1 in $P6_3mc$) together with both itself and copies of this cell produced by inversion. Figure 9 shows the result of linking the cell with its inverted copy. This clearly adds a center of symmetry where the cells link together. In this case it produces a molybdenum sheet on either side of the central Mo_6O_{18} cluster. However, if the inverted unit was added to the bottom of the original unit shown in Figure 2 it would produce a central unit with La sheets as the nearest neighboring sheets on both sides of the central Mo_6O_{18} cluster. Introducing stacking faults produces a disordered structure which appears on average to have $P6_3/mmc$ symmetry.

High-resolution electron microscopy might yield information on the number of stacking faults in $LaMo_2O_5$, but the difference in contrast between the layers will make this a difficult task. Electron microscopy will give no additional information on bond lengths and cluster types. We believe that a more profitable line of research is to determine atomic correlation functions using total neutron scattering.[26] This will enable us to further test the validity of our model.

Conclusions

$LaMo_2O_5$ contains the second known example of an isolated Mo_6O_{18} cluster and a new type of Mo−Mo bonded sheet formed from fused Mo_3 triangles. The structure is disordered, but is described as being built from ordered structural units. We show how disorder in stacking these units together produces on average a centrosymmetric structure, which describes the Bragg scattering.

The final model is supported by bond order and contact considerations, and by EXAFS measurements, which yield local structural information. Although these cannot provide definitive proof that an alternative model cannot be produced to describe the average structure, we were unable to do so. We propose to test our model further using total neutron scattering.

Acknowledgment. S.P. thanks TUBITAK/Turkey for a grant, S.P.C. thanks the EPSRC for a studentship, and we thank the EPSRC for allocation of neutron beam time.

Supporting Information Available: Listings of intensity and estimated standard deviations against time-of-flight and *d* spacing (20 pages). Ordering information is given on any current masthead page.

IC980313J

(25) Hibble, S. J.; Cheetham, A. K.; Köhler, J.; Simon, A. *J. Less Common Metals* **1989**, *154*, 271.
(26) Hibble, S. J.; Fawcett I. D.; Hannon, A. C. *Inorg. Chem.*, **1997**, *36*, 1749.